PHYSICAL REVIEW C VOLUME 17, NUMBER 2 FEBRUARY 1978

Quasielastic charge exchange in $n^2H \rightarrow pnn$ at 794 MeV*

B. E. Bonner, J. E. Simmons, and J. M. Wallace
Los Alamos Scientific Laboratory, University of California, Los Alamos, New Mexico 87545

M. L. Evans,† G. Glass, J. C. Hiebert, Mahavir Jain,† and L. C. Northcliffe
Texas A & M University, College Station, Texas 77843

C. W. Bjork‡ and P. J. Riley
University of Texas, Austin, Texas 78712

C. G. Cassapakis§
University of New Mexico, Albuquerque, New Mexico 87131
(Received 5 August 1977)

The proton spectrum resulting from 794-MeV neutron bombardment of deuterium was measured at several angles. The angular distribution of the integral of the quasielastic charge exchange peak is fitted very well by the two exponential form $d\sigma/dt = \alpha_1 e^{\beta_1 t} + \alpha_2 e^{\beta_2 t}$ as has previously been found for the np elastic case. The ratio of the two cross sections at $t = 0$ is 0.56 ± 0.04. A modified impulse approximation calculation accounts for most features of the observed angular distribution.

[NUCLEAR REACTION $n^2H \rightarrow pnn$, $E = 794$ MeV; measured $\sigma(\theta)$. Calculated $\sigma(\theta)$ with modified PWIA.]

I. INTRODUCTION

Few measurements exist relating to the quasielastic (QE) charge exchange (CEX) reaction on deuterium ($n^2H \rightarrow pnn$ and $p^2H \rightarrow npp$) at medium energy. Near 150 MeV[1,2] it is known that the 0° spectrum of the detected nucleon consists of a sharp peak [full width at half maximum (FWHM) ~2 MeV] with an energy near that of the beam and a small number of lower energy particles. At larger angles the peak broadens until the width approaches that expected from the Fermi momentum distribution of the struck nucleon inside the deuteron. The narrow peak at small angles is generally attributed to kinematics of quasifree scattering and to the $^1S_0$ final state interaction of the undetected nucleons. In an earlier measurement[3] the peak width at 730 MeV was found to be ~19 MeV FWHM at 8°. We recently reported a measurement[4] of the 0° neutron spectrum from 800-MeV protons on deuterium in which the peak width was determined to be ~10 MeV.

The QECEX cross section is obtained by integrating over the peak of the measured spectrum. It has been found that the ratio of this cross section near 0° (lab) to the elastic CEX cross section ($np \rightarrow pn$) is in the range of 0.5 to 0.7[1,3,4] although one such measurement[5] yielded a value of 0.2 ± 0.035 at 380 MeV. At 152 MeV[1] it was found that this ratio increases with angle and reaches unity near 30° lab. Statistical errors were 10% to 15% for this measurement, however. It was pointed out[6] as long ago as 1951 that this ratio is expected to be less than unity because of the suppression of allowed final states due to the operation of the Pauli principle in the QE case. The magnitude of the ratio is determined by the spin dependence at small momentum transfers in np scattering. Using the impulse approximation and certain simplifying assumptions, it can be related to the ratio of singlet to triplet amplitudes. Therefore, one might expect to be able to extract new information on the spin dependence of the np interaction from measurements on the quasielastic charge exchange reactions.

In the present paper we report a measurement of the QE differential cross section at laboratory angles from 0° to 18° resulting from 794-MeV neutron bombardment of deuterium. In Sec. II we give a brief description of the experiment, Sec. III contains our experimental results, in Sec. IV we compare our results with a theoretical calculation, and some conclusions are presented in Sec. V.

II. DESCRIPTION OF EXPERIMENT

The nearly monoenergetic (~10 MeV FWHM) neutron beam and spectrometer system used in

the present experiment has been described previously.[4,7,8] Briefly, the 800-MeV, 1-μA proton beam from the Clinton P. Anderson Meson Physics Facility (LAMPF) passed through a 10.6-cm-thick liquid deuterium target and was then bent through 60° and buried in a remote beam stop. Neutrons emerging at 0° were collimated to a half-angle of 0.1° and after being cleared of charged particles, encountered a 12.6-cm-thick liquid deuterium target placed upstream of a multiwire proportional chamber spectrometer. The momenta and flight times of charged particles emerging from this target into the acceptance of the spectrometer were measured. The momentum resolution $\Delta P/P$ was about 1% FWHM. Particle identification was unambiguous for more than 99% of the events. Absolute normalization of the cross sections was obtained from a separate measurement of the np CEX cross section at 800 MeV.[7] The overall uncertainty in the absolute cross sections is ±8%, resulting primarily from the uncertainty in the cross section for the normalizing reaction, $np \rightarrow D\pi^0$.

Measurements were made for four angular settings of the spectrometer: 0°, 4°, 8° and 16°. The angular acceptance of the spectrometer was about 4°, and the angular resolution was about ±2 mrad including the effects of multiple Coulomb scattering. The statistical accuracy of the proton spectra is excellent since they were obtained while measuring concurrently the much lower cross section for nD elastic scatterings.

III. EXPERIMENTAL RESULTS

The proton spectrum observed at each of the nominal spectrometer angle settings, integrated over the acceptance of the spectrometer, is shown in Fig. 1. The sharp peak observed at 0° is seen to broaden gradually with increasing angle. At each angle the peak is well defined and its centroid is located at a momentum consistent with free np elastic scattering. At 16° the width of the peak is consistent with that calculated from the Fermi momentum distribution of the struck nucleon in the deuteron folded with kinematic and cross section variation across the finite acceptance of the spectrometer. At smaller angles the $^1S_0$ final state interaction between the two unobserved neutrons and kinematical constraints combine to sharpen the peak dramatically.

In order to study the angular distribution of the quasielastic CEX cross section, the data were sorted into 0.005-rad bins and the peaks were integrated to give a cross section for each angle. Setting the limits of integration posed a problem since the width of the peak increases substantially with angle. The upper limit was easily set since there were no protons with momentum greater than those of interest. In order to have a consistent lower limit as a function of angle, the following prescription was used: protons falling below the momentum of a proton elastically scattered by a neutron of 730 MeV were rejected. The lower limit is indicated on each spectrum in Fig. 1 for the nominal spectrometer angle value. This prescription has the desired effect of including all the peak at all angles. This prescription is also incorporated in the modified plane-wave–impulse-approximation (PWIA) calculation to be described below. Center-of-mass cross sections were calculated for the central incident neutron energy of 794 MeV and then converted to $d\sigma/dt$, where t is the square of the four-momentum transferred between the incident neutron and the detected proton.

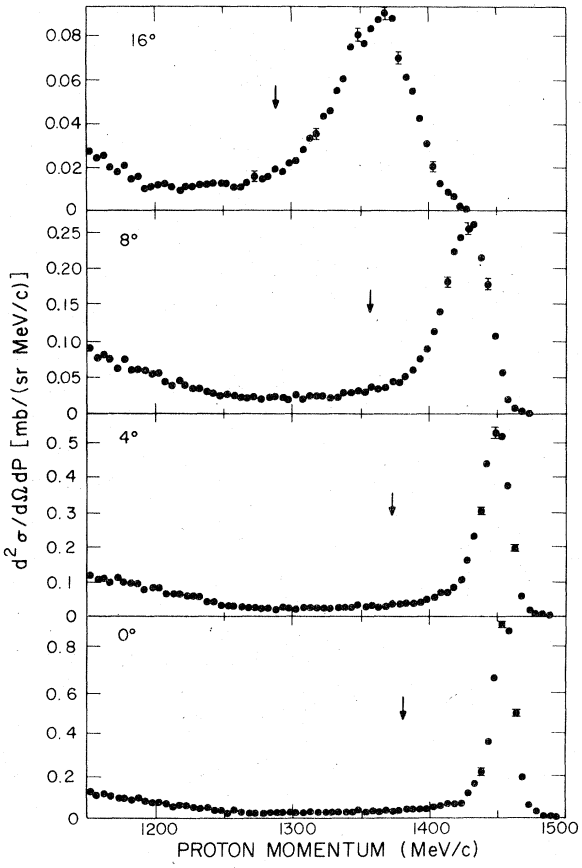

FIG. 1. Proton spectra observed at spectrometer angles of 0°, 4°, 8°, and 16° from the reaction $n^2H \rightarrow p$ at 794 MeV. The average angle over which protons are detected is dependent on the proton momentum for a given spectrometer setting (Ref. 7). For the central values of the peaks in the four spectra, the average angles are 1.3°, 4.4°, 8.1°, and 15.2°.

The values so obtained are plotted as a function of $-t$ in Fig. 2 and tabulated in Table I. For the spectrometer setting of 0°, particles detetected on opposite sides of the beam direction were kept separate to check for instrumental asymmetries and are also separated in the table. Also plotted in Fig. 2 are the 152-MeV QECEX data and elastic CEX given in Ref. 1 (divided by five for plotting convenience). It is apparent that a qualitatively similar behavior is observed at the two energies, but the present data are of higher statistical precision.

It is known[9,10] for free np CEX that the t variation of the cross section is described over a wide range of incident energies by a simple sum of two exponentials: $d\sigma/dt = \alpha_1 e^{\beta_1 t} + \alpha_2 e^{\beta_2 t}$. We have fitted the present data with this function and find that the quasielastic np CEX is also well represented by this function. Table II lists the values of these parameters found in the present experiment. Also listed are values for the free CEX cross section as determined for two sets of data[7,9] at nearby energies. The solid line through our data points in Fig. 2 is a plot of the fit to our data while the dashed line above is the fit to the free CEX Saclay data.[9] The quality of the fit to the QE data is indicated by the value of χ^2/ν which is 1.46.

From the fits obtained we can derive the ratio of the quasielastic CEX cross section at $t = 0$ to the elastic cross section. This ratio is 0.56 ± 0.04 at 794 MeV. In our previously reported 0° measurement[4] on the charge conjugate reaction $pD \to npp$, the value obtained for this quantity was

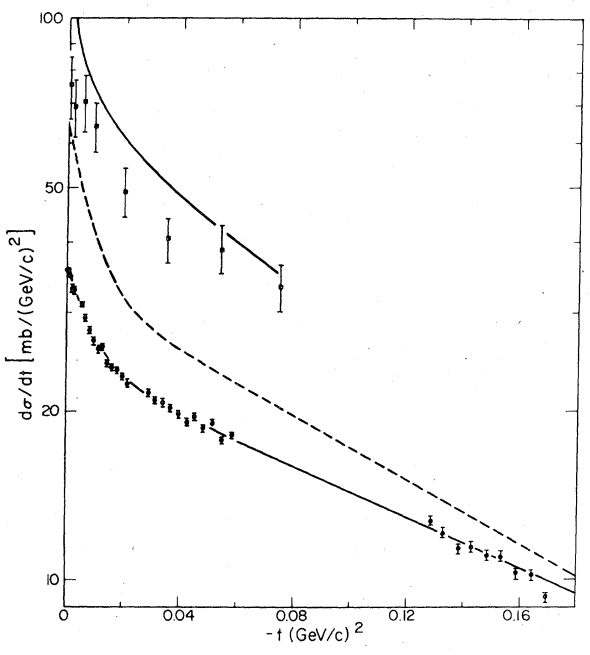

FIG. 2. Quasielastic CEX ($nD \to pnn$) compared to elastic CEX at 794 MeV. Present results (solid circles) compared with the fit to Ref. 9 elastic CEX results (dashed line). The solid line through our data points is the result of the double exponential fit (see text). Results at 152 MeV (Ref. 1) (solid squares) QECEX and elastic CEX (upper solid line) have been divided by five.

TABLE I. Cross sections for $nD \to pnn$ at 794 MeV. Stated errors are those due to counting statistics only. An additional ±8% normalization error is not included (see text).

$-t$ (GeV/c)^2	$d\sigma/dt$ [mb/(GeV/c)^2]
0.001 672[a]	35.61 ± 0.49
0.001 131[a]	36.40 ± 0.48
0.000 696[a]	36.52 ± 0.47
0.000 366[a]	37.34 ± 0.44
0.000 142[a]	37.53 ± 0.52
0.000 023[a]	37.23 ± 0.69
0.000 068	37.40 ± 1.37
0.000 119	39.10 ± 0.93
0.000 314	38.22 ± 0.60
0.000 620	36.50 ± 0.47
0.001 031	36.57 ± 0.44
0.001 549	35.31 ± 0.47
0.002 172	33.93 ± 0.47
0.002 869	33.69 ± 0.50
0.005 773	31.75 ± 0.35
0.006 928	30.11 ± 0.34
0.008 186	28.58 ± 0.33
0.009 549	27.38 ± 0.33
0.011 016	26.47 ± 0.32
0.012 586	26.76 ± 0.32
0.014 259	25.05 ± 0.31
0.016 035	24.60 ± 0.31
0.017 913	24.22 ± 0.31
0.019 893	23.64 ± 0.31
0.021 812	22.99 ± 0.33
0.028 956	22.16 ± 0.27
0.031 445	21.49 ± 0.27
0.034 032	21.26 ± 0.27
0.036 717	20.85 ± 0.27
0.039 500	20.29 ± 0.26
0.042 381	19.60 ± 0.26
0.045 358	20.06 ± 0.26
0.048 431	19.14 ± 0.26
0.051 599	19.49 ± 0.26
0.054 861	18.22 ± 0.25
0.058 218	18.64 ± 0.25
0.128 318	13.07 ± 0.25
0.133 214	12.43 ± 0.25
0.138 188	11.65 ± 0.24
0.143 239	11.72 ± 0.24
0.148 364	11.30 ± 0.27
0.153 565	11.28 ± 0.24
0.158 838	10.53 ± 0.23
0.164 184	10.44 ± 0.23
0.169 602	9.60 ± 0.22

[a]These values refer to protons scattered to the left at 0°, while the others are for right-scattered protons.

TABLE II. Parameter values for elastic and quasielastic np CEX. Quoted errors are derived from statistical errors only.

	$d\sigma/dt = \alpha_1 e^{\beta_1 t} + \alpha_2 e^{\beta_2 t}$		
Parameter	Quasielastic Present expt.	Elastic Saclay[a] (814 MeV)	Elastic Los Alamos[b] (800 MeV)
α_1	12.87 ± 0.22	32.48	34.46
β_1	123.4 ± 5.1	122.0	150.0
α_2	25.11 ± 0.17	33.30	33.51
β_2	5.38 ± 0.08	6.61	6.08
$d\sigma/dt$ $(t=0)$ $(=\alpha_1+\alpha_2)$	37.98 ± 0.70	65.78	67.97

[a] Reference 9.
[b] Reference 7.

0.66 ± 0.08. Many of the sources of error present in that experiment do not occur in the present measurement.

IV. IMPULSE APPROXIMATION CALCULATIONS

In this section we present a plane-wave–impulse-approximation (PWIA) analysis of the cross section $d\sigma/d\Omega_p$ for the reaction $nD \to ppn$ at 794 MeV. The formulas used are essentially generalizations of those previously derived by Chew.[6,11] The notation followed is that of Ref. 16. As input we employ the nucleon-nucleon phase shifts of MacGregor, Arndt, and Wright (MAW),[12] together with the parametrization of the 800-MeV np CEX cross section from Ref. 7. In Fig. 3 the parametrization of these data is compared with the prediction from the phase shifts at 750 MeV. The lack of agreement does not significantly affect our subsequent evaluations, as is shown in Sec. IV B. The np parameters that were used are given in Table II, column 3 and were derived from the data of Ref. 7. For a deuteron wave function, we have employed the best Moravcsik fit[13] to the Gartenhaus wave-function,[14] which has proved satisfactory in analyses of nucleon-deuteron scattering data in the past.[15,16] Recent developments[17] at high momentum transfers have negligible influence on the part of the deuteron wave function probed by the present experiment.

A. Derivation of the PWIA formulas

In the PWIA one describes the quasielastic nD process as essentially a single interaction of the projectile with the bound proton constituent of the deuteron as is shown diagrammatically in Fig. 4. Denoting by Ω_p the solid angle into which the proton is scattered and assuming the deuteron initially at rest, the laboratory differential cross section for a fast proton in the final state is

$$\frac{d\sigma}{d\Omega_p} = \frac{1}{6} \sum_{\text{spins}} \int d^3k_{n2} K |\langle g | T | i \rangle|^2, \tag{1}$$

where $\langle g| = 1/\sqrt{2}\,(\langle f| - \langle f'|)$ is the antisymmetrized final state, $\langle f|$ differing from $\langle f'|$ only in that neutrons 1 and 2 are interchanged. The kinematic factor is given by

$$K = \frac{k_p^2}{32(2\pi)^5 p_{n1} M E(k_{n2}) \,|\, k_p E(k_{n1}) + [k_p + \hat{k}_p \cdot (\vec{k}_{n2} - \vec{p}_{n1})] E(k_p) \,|},$$

where $E(k) = (k^2 + m^2)^{1/2}$ are the nucleon energies and M is the deuteron mass.

The nD scattering amplitude in PWIA may be written explicitly as

$$\langle f | T | i \rangle = (2\pi)^{3/2} (2M)^{1/2} \times \langle L | T_{np}(\vec{p}_{n1}, -\vec{k}_{n2} - \vec{k}_{n1}, \vec{k}_p) \phi(\vec{k}_{n2}) | s \rangle, \tag{2}$$

where $\phi(\vec{q})$ is the deuteron internal wave function in spin and momentum space, $\langle L|$ is the three-particle spin state, and $|s\rangle$ is the projectile neutron spin state.

T_{np} is related to the np center-of-mass (c.m.) differential cross section by

$$\left(\frac{d\sigma}{d\Omega_{n\to n'}}\right)^{np}_{\text{c.m.}} = \frac{1}{(8\pi W)^2} \times |\langle n' | T_{np}(\vec{p}_n, \vec{p}_p \to \vec{k}_n, \vec{k}_p) | n \rangle|^2, \tag{3}$$

where $|n\rangle$ and $|n'\rangle$ are, respectively, the initial and final np spin states and W is the center-of-mass energy.

Substituting Eq. (2) into Eq. (1) we obtain

$$\frac{d\sigma}{d\Omega_p} = \frac{1}{6} \sum_{\text{spins}} \int d^3k_{n2} \frac{k_p^2}{(8\pi)^2 p_{n1} E(k_{n2}) \,|\, k_p E(k_{n1}) + [k_p + \hat{k}_p \cdot (\vec{k}_{n2} - \vec{p}_{n1})]\, E(k_p) \,|} \times \tfrac{1}{2} \,|\langle L | T_{np}(\vec{p}_{n1}, -\vec{k}_{n2} - \vec{k}_{n1}, \vec{k}_p) \phi(\vec{k}_{n2}) | s \rangle - \langle L' | T_{np}(\vec{p}_{n1}, -\vec{k}_{n1} - \vec{k}_{n2}, \vec{k}_p) \phi(\vec{k}_{n1}) | s \rangle|^2. \tag{4}$$

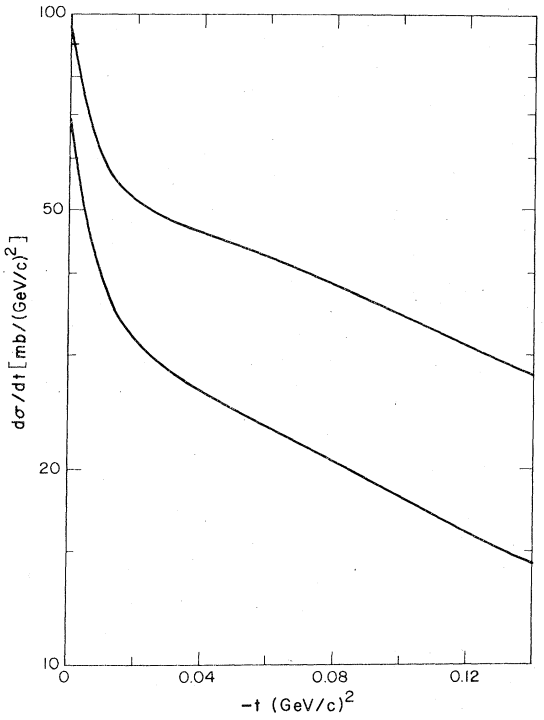

FIG. 3. Parametrization of the Los Alamos 800-MeV np CEX data (lower curve) reported in Ref. 7 compared with the prediction extrapolated from the previously existing MAW phase shifts (Ref. 12) (upper curve.)

Some simplifying kinematical approximations in Eq. (4) can be made. Except for the arguments of the deuteron wave functions, which are the only rapidly varying quantities under the integral, we assume that all momenta may be replaced by the corresponding momenta for free np CEX scattering at the same proton scattering angle off a stationary proton target. With this approximation, subsequent to spin summation, Eq. (4) simplifies to

$$\frac{d\sigma}{d\Omega_p} = \left(\frac{d\sigma}{d\Omega_p}\right)^{np} - S_0(\Delta)\left(\frac{d\sigma}{d\Omega_p}\right)^{e1} - S_2(\Delta)\left(\frac{d\sigma}{d\Omega_p}\right)^{e2} \tag{5}$$

where the laboratory cross sections can be expressed in terms of the c.m. cross sections

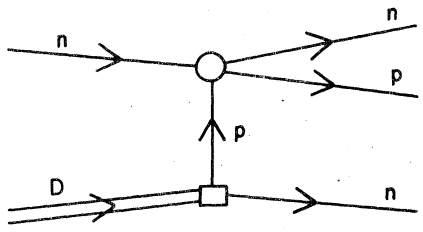

FIG. 4. Diagrammatic representation of the PWIA for $nd \to pnn$.

by

$$\left(\frac{d\sigma}{d\Omega_p}\right)^{np}_{\text{c.m.}} = \frac{p_{n1}\, m\, |k_p E(k_{n1}) + (k_p - \hat{k}_p \cdot \vec{p}_{n1}) E(k_p)|}{k_p^{\,2} W^2} \times \left(\frac{d\sigma}{d\Omega_p}\right)^{np}_{\text{lab}} (\vec{p}_{n1}, \vec{0} \to \vec{k}_{n1}, \vec{k}_p) ,$$

with similar expression for $(d\sigma/d\Omega_p)^{e1}$ and $(d\sigma/d\Omega_p)^{e2}$.

The c.m. differential cross sections for np scattering can be written in the notation of Stapp, Ypsilantis, and Metropolis[18] as

$$\begin{aligned}
\left(\frac{d\sigma}{d\Omega_p}\right)^{np}_{\text{c.m.}} &= \tfrac{1}{2}\,|M_{11}|^2 + \tfrac{1}{4}|M_{00}|^2 + \tfrac{1}{2}|M_{10}|^2 \\
&\quad + \tfrac{1}{2}|M_{01}|^2 + \tfrac{1}{2}|M_{1,-1}|^2 + \tfrac{1}{4}\,|M_{ss}|^2 , \\
\left(\frac{d\sigma}{d\Omega_p}\right)^{e1}_{\text{c.m.}} &= \tfrac{1}{3}|M_{11}|^2 + \tfrac{1}{8}|M_{00}|^2 + \tfrac{1}{4}\,|M_{01}|^2 \\
&\quad + \tfrac{1}{4}\,|M_{10}|^2 + \tfrac{1}{6}|M_{1,-1}|^2 + \tfrac{1}{6}\,\mathrm{Re}(M_{00}M_{11}^*) \\
&\quad - \tfrac{1}{6}\,\mathrm{Re}(M_{01}M_{10}^* e^{-2i\phi}) - \tfrac{1}{6}\,\mathrm{Re}(M_{11}M_{ss}^*) \\
&\quad - \tfrac{1}{12}\,\mathrm{Re}(M_{00}M_{ss}^*) + \tfrac{1}{8}\,|M_{ss}|^2 , \\
\left(\frac{d\sigma}{d\Omega_p}\right)^{e2}_{\text{c.m.}} &= -\tfrac{1}{3}\,|M_{11}|^2 + \tfrac{1}{3}|M_{1,-1}|^2 + \tfrac{1}{3}\,\mathrm{Re}(M_{00}M_{11}^*) \\
&\quad + \tfrac{1}{3}\,\mathrm{Re}(M_{00}M_{ss}^*) - \tfrac{1}{3}\mathrm{Re}(M_{11}M_{ss}^*) \\
&\quad - \tfrac{1}{3}\mathrm{Re}(M_{01}M_{10}^* e^{-2i\phi}) .
\end{aligned} \tag{6}$$

The M_{lm} are c.m. np amplitudes with $l, m = 1, 0, -1$ indicating initial and final spin projections in the triplet system and $l = m = s$ indicating the singlet amplitude. The azimuthal c.m. scattering angle is denoted by ϕ. The first term in Eq. (5) is simply the corresponding free np scattering cross section, and $\Delta = |\vec{p}_{n1} - \vec{k}_p|$ is the magnitude of the vector momentum transfer. The charge and quadrupole deuteron form factors S_0 and S_2 are defined in Ref. 15.

The second and third terms of Eq. (5), which arise from the cross terms of Eq. (4), contain the effects of the Pauli exclusion principle. These terms are most important in suppressing the $nD \to pnn$ cross section at low momentum transfers where both neutrons emerge with low relative energy and are thus quite close together in momentum space. The terms give a negative contribution which is 36% of the first term at $t = 0$. As the momentum transfer increases, the final-state neutrons need not be as close together and the Pauli terms diminish in importance, giving only a negative 1% contribution at the largest momentum transfer considered here.

At low energies and small Δ, Eq. (5) reduces to a formula previously derived by Chew.[6] The reduction is obtained by (1) assuming the deuteron is pure S state so $S_2 \equiv 0$, a low-Δ approximation; (2) assuming $M_{lm} = \delta_{lm} M_{tt}$ in the triplet channel, a low-

energy approximation.

Unfortunately Eq. (5) cannot be applied directly to the present experiment because for a given scattering angle, only protons with momenta larger than $(k_p)_{min}$ are observed as described in Sec. III. When three-body energy and momentum conservation are taken into account, it is found that the higher momentum components of the deuteron wave function correspond to $k_p < (k_p)_{min}$ and hence do not contribute to the observed cross section $d\sigma/dt$. To calculate the observed cross sections properly, one should go back to Eq. (4) and cut off the k_{n2} integration appropriately. Instead of carrying this out in its entirety, we have developed an approximation which enables us to use the much simpler Eq. (5) with only a simple modification.

We perform a numerical integration of Eq. (4), with the proper cutoff, neglecting the cross terms of the two matrix elements. The ratio, denoted by $R(\Delta)$, of this result to the first term of Eq. (5) (which is essentially the above integration without the cutoff) is then calculated. Finally the entire right hand side of Eq. (5) is simply multiplied by $R(\Delta)$, which is a relatively small correction ranging from $R=0.934$ at $t=0$ to $R=0.757$ at $t=-0.156$ (GeV/c)^2.[19] The first term of Eq. (5), the numerically dominant term, is thus replaced by the corresponding exact expression. At small momentum transfers, where the second and third terms are most important, the correction is rather accurate, becoming exact at $t=0$. While the correction becomes less accurate at higher momentum transfers, these terms become less important. The correction procedure is expected to be quite satisfactory over the entire momentum transfer range considered. Moreover, this modification of Eq. (5) also compensates for the small errors introduced by the kinematical approximations made earlier.

B. Application

The formula used to calculate $d\sigma/d\Omega_p$ is

$$\frac{d\sigma}{d\Omega_p} = \left[\left(\frac{d\sigma}{d\Omega_p}\right)^{np} - S_0(\Delta)\left(\frac{d\sigma}{d\Omega p}\right)^{e1} - S_2(\Delta)\left(\frac{d\sigma}{d\Omega_p}\right)^{e2}\right] R(\Delta)\,, \tag{7}$$

where $d\sigma/d\Omega_p$ is transformed to $d\sigma/dt$ in the same way as the experimental data. The form factors in Eq. (7) are obtained from numerical integration of the Gartenhaus deuteron wave function. The cross sections are calculated using the 750-MeV MAW phase shifts and are rescaled using the ratio

$$\left(\frac{d\sigma^{np}}{dt}\right)^{800\ \text{MeV}}_{\text{observed}} \Big/ \left(\frac{d\sigma^{np}}{dt}\right)^{750\ \text{MeV}}_{\text{phase shifts}}$$

Thus, the cross section in the leading term is essentially exact; the discrepancy between the two

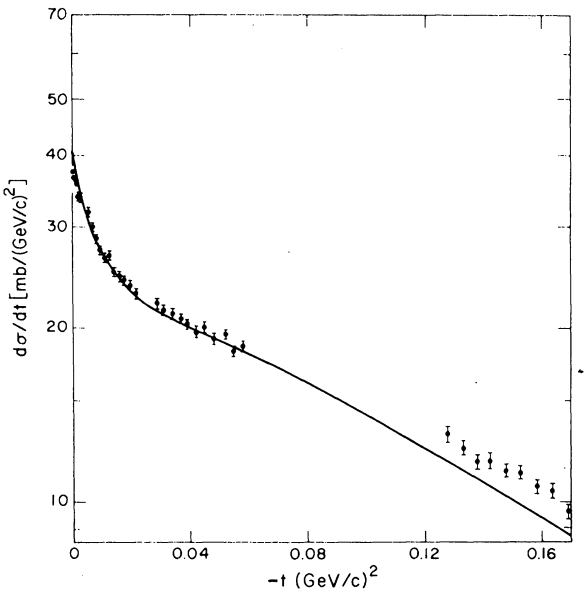

FIG. 5. Quasielastic CEX ($n^2H \rightarrow pnn$) (dark circles) compared with impulse approximation calculation (solid line).

curves in Fig. 3 is removed. There is some unavoidable uncertainty in the exchange cross sections as no reliable phase shift analysis extending through the 800-MeV region currently exists.

In the $R(\Delta)$ calculation the T_{np} matrix was evaluated at the final energy of the two particles. The on-shell np differential cross section is taken[10] to vary with energy as P_{lab}^{-2} around the 800-MeV value given in Sec. III.

The results of the PWIA calculation are compared with the data in Fig. 5. The calculation is within ~14% of the present experiment at all momentum transfers, with the largest discrepancies occurring at the largest $-t$ values. It is quite possible that in this large momentum transfer region multiple scattering effects analogous to those in pD elastic scattering[15] are beginning to manifest themselves. A more refined analysis might take these processes into consideration.

V. CONCLUSION

We have reported a measurement on the quasielastic charge exchange reaction $nD \rightarrow pnn$ at 794 MeV. The spectrum of high momentum protons from this reaction broadens smoothly with angle and the integral of the observed peak decreases with angle in a manner similar to the free np charge exchange cross section. Using the phase shifts of MacGregor, Arndt, and Wright as input to a modified plane-wave–impulse-approximation calculation, we are able to fit, within the experimental normalization uncertainty, the small

$-t$ behavior of the cross section. This implies that the phase shifts predict rather accurately the ratio of the exchange cross section (particularly the more important exchange cross section, $e1$) to the elastic cross section. The lack of agreement at larger values of $-t$ cannot be attributed to these phase shift uncertainties since the exchange cross section contributions are very small for large $-t$. A more likely explanation for the large $-t$ discrepancy is that multiple scattering effects are responsible. Because the $nD \to pnn$ reaction is amenable to a rather straightforward analysis, at least at very low momentum transfers, it may well be useful as an additional constraint in future $T = 0$ phase shift analyses.

ACKNOWLEDGMENTS

We would like to thank the staff of LAMPF for their help essential to the performance of this experiment. Special thanks are due Ken Williamson, Jr., for assistance with the cryogenic apparatus, Anne Niethammer for help with programming, and to both Professor Howard Bryant and Jan Boissevain for their many contributions.

---

*Work performed under the auspices of the U. S. Energy Research and Development Administration.

†Present address: Los Alamos Scientific Laboratory, University of California, Los Alamos, New Mexico 87545.

‡Present address: University of Wyoming, c/o LAMPF Visitors Center, Los Alamos, New Mexico, 87545.

§Present address: Science Applications, Inc., La Jolla, California 92037.

[1]D. F. Measday, Phys. Lett. 21, 66 (1966); Phys. Rev. 142, 584 (1966).

[2]A. Langsford *et al.*, Nucl. Phys. A99, 246 (1967).

[3]R. R. Larsen, Nuovo Cimento 18, 1039 (1960).

[4]C. W. Bjork *et al.*, Phys. Lett. 63B, 31 (1976).

[5]V. P. Dzhelepov *et al.*, Suppl. Nuovo Cimento 3, 61 (1956).

[6]G. F. Chew, Phys. Rev. 84, 710 (1951).

[7]M. L. Evans *et al.*, Phys. Rev. Lett. 36, 497 (1976). This reference contains np results from this group at 647 MeV and gives a description of the techniques used. Our preliminary data at 800 MeV used in the present calculation are given in: L. C. Northcliffe, in Proceedings of the International Conference on Interactions of Neutrons with Nuclei, Lowell, Mass., 1976 (unpublished), ERDA-760715.

[8]C. G. Cassapakis *et al.*, Phys. Lett. 63B, 35 (1976).

[9]G. Bizard *et al.*, Nucl. Phys. B85, 14 (1975).

[10]B. E. Bonner *et al.*, in Proceedings of the Second International Conference on the N-N Problem, Vancouver, 1977 [A.I.P. (to be published)].

[11]G. F. Chew, Phys. Rev. 80, 196 (1950).

[12]M. H. MacGregor, R. A. Arndt, and R. M. Wright, Phys. Rev. 169, 1149 (1968); 173, 1272 (1968).

[13]M. J. Moravcsik, Nucl. Phys. 7, 113 (1958).

[14]S. Gartenhaus, Phys. Rev. 100, 900 (1955).

[15]V. Franco, R. J. Glauber, Phys. Rev. Lett. 22, 370 (1969).

[16]J. M. Wallace, Phys. Rev. C 5, 609 (1972).

[17]M. Gari and H. Hyuga, Phys. Rev. Lett. 36, 345 (1976), and references cited therein.

[18]H. P. Stapp, T. J. Ypsilantis, and N. Metropolis, Phys. Rev. 105, 302 (1957).

[19]There is no reason why the cross terms in Eq. (4) could not be integrated numerically. The terms are somewhat less tractable involving products of np amplitudes calculated at different energies and angles instead of simply an np differential cross section. It is doubtful that much would be gained in carrying out this calculation, particularly since the required amplitudes are not well known in the vicinity of 800 MeV.